# Molecular dynamics of detonation. I. Equation of state and Hugoniot curve for a simple reactive fluid

Jerome J. Erpenbeck
*Los Alamos National Laboratory, Los Alamos, New Mexico 87545*
(Received 11 June 1992)

A simple microscopic model of chemical reactions is explored for diatomic exchange reactions $2AB \rightleftharpoons A_2 + B_2$. A pair of atoms bind chemically when they lie within a "square" attractive well. The presence of a bond, however, leaves the bound atoms in a state in which they have only hard-sphere repulsion for other atoms. A calculation combining the canonical-ensemble Monte Carlo technique with molecular dynamics is used to determine the equilibrium composition and thermodynamic properties of equimolar binary mixtures of $A$ and $B$ atoms, subject to this square-well, hard-sphere interaction potential for temperatures and densities accessible to detonation waves in a fluid consisting of metastable $AB$ molecules at an initial temperature $\varepsilon_{AB}/20k_B$ (in which $\varepsilon_{ab}$ is the well depth of the $ab$ interaction and $k_B$ is the Boltzmann constant), with $\varepsilon_{AA} = 3\varepsilon_{AB}$ and $\varepsilon_{BB} = \varepsilon_{AB}$. The calculations for systems of both 216 and 1728 atoms include the pressure, the internal energy, and the mean free times for various types of collisions. The Hugoniot curve for states behind detonation waves is determined for six values of the density for the smaller systems and one value for the larger; finite-system effects are found to be small. The Hugoniot curve is shown to have a concave shape in the pressure-volume plane, typical of exothermic materials, and the Chapman-Jouguet state is determined.

PACS number(s): 47.40.−x, 47.70.Fw, 82.60.Hc, 03.40.Kf

## I. INTRODUCTION

The classical hydrodynamic theory of detonation [1] presents a remarkably simple picture of a detonation wave, based on the so-called Chapman-Jouguet (CJ) hypothesis and simple, one-dimensional conservation relations, as expressed in the Euler equations. Nonetheless, that theory seems only partially relevant to the observed phenomenon of detonation for two distinct reasons. First, steady one-dimensional detonation waves, when viewed on the length and time scales defined by the chemical process, are found to be *unstable* for a variety of idealized, one-reaction detonations in gases [2–5] as well as for certain models of condensed-phase detonations [6]. In lieu, then, of an understanding of the time-dependent multidimensional flow, the connection between the theory and the experimental "fully developed detonation" is tenuous. Second, the *initiation* of detonation does not appear amenable to a strictly hydrodynamic explanation because certain physical properties at least of solid explosives, beyond the equation of state (such as grain size and crystal structure), are often of controlling importance. Indeed, little is known theoretically of the processes that control initiation.

Microscopic approaches to detonation, which have gained popularity in roughly the past decade, are aimed at understanding initiation. Classical molecular dynamics has been prominent among these approaches. Calculations by Karo, Hardy, and Walker [7], Tsai and Trevino [8], and Peyrard and co-workers [9–11] were based on so-called "predissociative potentials," in which a molecule of the explosive is represented as a dimer, bound in a metastable state through a barrier in the potential-energy function, the height of that barrier being large compared to the thermal energy in the quiescent (i.e., unshocked) explosive. While these models address the problem of providing for the exothermicity of the explosive, they ignore the fact that dissociation is an endothermic process. The energy of the explosive arises instead from the recombination reactions. Thus, the exothermic step should occur on a time scale no smaller than the mean free time rather than the scale of the duration of a collision inherent in the predissociative models.

In solids, however, this distinction in time scales becomes blurred and dissociation and recombination are now always separate steps. For this reason, the inadequacy of the predissociative potential seems to lie more in its oversimplification of the molecular processes involved. This point of view has been stressed in more recent treatments. These include a one-dimensional calculation for a nitric-oxide-like potential having the London-Eyring-Polyani-Sato form by Elert, Deaven, Brenner, and White [12]. The importance of the chemical dynamics has especially been stressed by Robertson, Brenner, Elert, and White [13], who have reported both one-dimensional and two-dimensional calculations for a reaction $2AB \rightarrow A_2 + B_2$ using a many-body Tersoff-type potential. A different approach has been taken by Lambrakos, Peyrard, Oran, and Boris [14] in a three-dimensional (non-Hamiltonian) calculation in which dimer bonds are constrained to fixed length through the equations of motion, at the same time calculating a phenomenological *state function* $S_{ij}(t)$ of each bond through the interatomic forces each of its atoms has experienced. When $S_{ij}$ exceeds some threshold, the bond is considered broken, the constraint is relaxed, and energy is released by replac-

 

ing the intramolecular constraint by a repulsive intermolecular potential energy of the dissociated atoms.

While the role for molecular dynamics in detonation physics would evidently lie in the initiation problem, as recognized by much of the previous work, the problem is of sufficient complexity that the significance of many of the observations that have been reported seems unclear. As noted above, from the hydrodynamic point of view detonations appear to be inherently multidimensional, in contrast to shock waves in inert materials, which have been studied with some success through molecular dynamics. Moreover, in the direction of propagation, it is expected that the wave needs to be followed in time and space over many reaction-zone lengths in order that transients should decay. Thus the denotation problem can be expected to require the treatment of a system of considerable length not only in the direction of propagation of the front but also in the transverse direction. In the case of solid explosives, for which reaction-zone lengths are expected to be rather short, one is faced with the need to deal with lattice imperfections whose size and concentration would also dictate the need to treat systems much larger than those needed, for example, in the molecular dynamics of the thermophysical properties of fluids. In short, the problem is fraught with difficulties on a scale unprecedented perhaps in molecular dynamics.

While attempts have been made to deal with the full complexity of the problem, the more common approach has been to reduce the complexity through the consideration of one- and two-dimensional systems and, following Peyrard *et al.* [10], to explicitly calculate the dynamics of only those particles lying within a "computational window" that is advanced along the direction of propagation in steps that are typically somewhat irregular in space and time. The effects of these simplifications have not been fully evaluated.

The present paper begins an attempt to evaluate the molecular dynamics of detonation by first determining quantitatively the predictions of the classical macroscopic theory. Rather than a solid, we consider a diatomic fluid in which the interaction potential of the chemically active atoms is both highly realistic, in that association and dissociation are strongly asymmetric three-body processes, and highly idealized, in that the potential is neither a fit to any particular substance nor the derivative a fundamental (quantum-mechanical) theory. Our ultimate aim is to study the hydrodynamic fields in shock-initiated flow in this idealized system and to compare these with the behavior inferred from classical detonation theory. While we are not aware of a theorem that the hydrodynamic theory necessarily holds in any particular region of state space, the failure or success of the theory in describing the molecular-dynamics (MD) results, coupled with observations of the validity of the fundamental hypothesis of that theory, viz., partial thermodynamic equilibrium, can be expected to shed considerable light on the utility of MD in the study of detonation.

In the present paper, we present our model and apply a combined Monte Carlo and molecular-dynamics method to determine the equilibrium composition and the equation of state from which we generate the Hugoniot curve, which plays a central role in the classical, Chapman-Jouguet theory of detonation. The present calculations differ from the approach taken by Coker and Watts [15] and Kofke and Glandt [16] in the determination of chemical equilibrium by virtue of our use of a reactive interaction potential. These previous approaches are based on Monte Carlo calculations in a restricted grand canonical ensemble, in which one specifies the chemical species that are present through an atom-in-molecule interaction potential. A similar Monte Carlo approach has been devised by Shaw [17] using a generalized canonical or constant-pressure ensemble in which the changes in composition are accomplished through atomic interchanges rather than the molecular moves of the previous work. The present approach is similar to that of Stillinger, Weber, and LaViolette [18] in the study of polymerization of liquid sulfur.

In Sec. II, we present the details of the model. In Sec. III, we consider the calculation of the thermodynamic functions, particularly as they apply to our impulsive-interaction model. We specify the interaction parameters and thermodynamic state for the calculations reported here in Sec. IV, along with certain details of our numerical calculations. We present our results in Sec. V and close with a brief discussion in Sec. VI.

## II. SYSTEM

We consider an "equimolar" mixture of $A$ and $B$ atoms, having masses $m_A$ and $m_B$ respectively, $N/2$ of each, at thermodynamic temperature $T$ and specific volume $v$ contained in a parallelopiped having edge length $L_x$, $L_y$, and $L_z$ along the three Cartesian axes, so that $v=2L_xL_yL_z/N(m_A+m_B)$. These atoms can associate into diatomic molecules $AB$, $AA$, and $BB$, which can also decompose. The dynamics of these processes are governed by classical dynamics based on an interaction potential that should include three-body (or more) terms in order to realistically treat the case of chemical reaction [18].

### A. Square-well, hard-sphere interaction

Here we choose perhaps the simplest realistic model of chemical reaction, viz., a three-body interaction consisting of square-well "attraction,"

$$\phi_{ab}(\mathbf{r}_{ij})=\varepsilon_{ab}u^{(\mathrm{SW})}(r_{ij}/\sigma_{ab},K_{ab})\ ,$$
$$u^{(\mathrm{SW})}(x,K)=\begin{cases}\infty & \text{if } x<1\\ -1 & \text{if } 1\le x<K\\ 0 & \text{if } K\le x\ ,\end{cases} \tag{1}$$

between atom $i$ of species $s_i$ (either $A$ or $B$) and atom $j$ of species $s_j$ (where we simplify by letting $a\equiv s_i$ and $b\equiv s_j$, with $a,b\in\{A,B\}$), whose centers $\mathbf{r}_i$ and $\mathbf{r}_j$ are separated by a vector $\mathbf{r}_{ij}=\mathbf{r}_i-\mathbf{r}_j$, provided neither $i$ nor $j$ lies within the attractive well of a third atom. When any pair of atoms lie in their attractive well, viz., $\sigma_{ab}\le r_{ij}<K_{ab}\sigma_{ab}$, they are said to form the $ab$ molecule. Atoms that are bound into molecules interact with other

atoms through a repulsive hard-sphere interaction, which we choose thus:

$$\phi_{ab}(\mathbf{r}_{ij}) = u^{(\mathrm{HS})}(r_{ij}/K_{ab}\sigma_{ab}) ,$$
$$u^{(\mathrm{HS})}(x) = \begin{cases} \infty & \text{if } x < 1 , \\ 0 & \text{if } 1 \le x . \end{cases} \tag{2}$$

The choice of the hard-sphere diameter to be equal to, rather than smaller than, the square-well diameter $K_{ab}\sigma_{ab}$ eliminates the possibility that the $i,j$ particles could discontinuously (in time) appear within (as opposed to at the boundary of) their attractive well at the instant a molecule involving $i$ or $j$, say $ik$, dissociates.

The potential energy of the system having configuration $\underline{r}^N = (\mathbf{r}_1, \mathbf{r}_2, \ldots, \mathbf{r}_N)$ can be written explicitly in terms of three-body contributions as follows:

$$U_N(\underline{r}^N) = \frac{1}{N-2} \sum_{i<j<k} \phi_{abc}(\mathbf{r}_i, \mathbf{r}_j, \mathbf{r}_k) ,$$
$$\begin{aligned} \phi_{abc}(\mathbf{r}_i, \mathbf{r}_j, \mathbf{r}_k) = {} & \varepsilon_{ab} u^{(\mathrm{SW})}\left[\frac{r_{ij}}{\sigma_{ab}}, K_{ab}\right] F_{ik}F_{jk} + u^{(\mathrm{HS})}\left[\frac{r_{ij}}{K_{ab}\sigma_{ab}}\right](1 - F_{ik}F_{jk}) \\ & + \varepsilon_{ac} u^{(\mathrm{SW})}\left[\frac{r_{ik}}{\sigma_{ac}}, K_{ac}\right] F_{ij}F_{jk} + u^{(\mathrm{HS})}\left[\frac{r_{ik}}{K_{ac}\sigma_{ac}}\right](1 - F_{ij}F_{jk}) \\ & + \varepsilon_{bc} u^{(\mathrm{SW})}\left[\frac{r_{jk}}{\sigma_{bc}}, K_{bc}\right] F_{ij}F_{ik} + u^{(\mathrm{HS})}\left[\frac{r_{jk}}{K_{bc}\sigma_{bc}}\right](1 - F_{ij}F_{ik}) , \end{aligned} \tag{3}$$

in which $c \equiv s_k$ and $F_{ij}$ is a unit-step function,

$$F_{ij} = A(r_{ij}/K_{ab}\sigma_{ab} - 1) .$$

[In writing Eq. (3), we understand the vanishing of an $F_{ij}$ factor to eliminate from the right-hand side of the equation the potential energy function $u$ that multiplies it, regardless of whether $u$ is infinite.]

The interaction potential simplifies somewhat when we impose additivity on the interaction lengths, so that we obtain the $\sigma_{ab}$ from the core diameter of the atoms,

$$\sigma_{ab} = \frac{\sigma_a + \sigma_b}{2} . \tag{4}$$

One could further reduce the potential parameters by imposing additivity on the square-well and hard-sphere interactions,

$$K_{ab}\sigma_{ab} = \frac{K_a\sigma_a + K_b\sigma_b}{2} ,$$

but we have not done so in the calculations reported here, choosing the $K_{ab}$ independently instead.

### B. Detonation model

We define a model for detonation based on the above interaction by considering a system consisting initially of metastable $AB$ molecules. That is, the thermal energy of the "quiescent" system is small compared to the well depth $\varepsilon_{AB}$, while the well depth for at least one of the other molecules is considerably larger, say $\varepsilon_{AA} \gg \varepsilon_{AB}$. The first condition assures that the quiescent, unshocked explosive will not decompose spontaneously and the second assures that considerable potential energy will be released in the formation of the $AA$ molecule.

Our overall aim is to study the development of detonation as, for example, a piston is moved into the system and a compression wave moves away from the piston, exciting chemical reaction through enhanced collision rates. We wish to compare the behavior of this microscopic system with that predicted by reactive hydrodynamics. In the present paper we are concerned principally with the hydrodynamic aspect of the problem at the level of the Chapman-Jouguet theory, which depends only on the equations of state of the quiescent explosive and the equilibrium mixture behind the zone of chemical change.

For the interaction potential Eq. (3) our aim, then, is to determine the equilibrium equation for state. For the present case, in which we have a reactive interaction potential, the classical methods of Monte Carlo and molecular dynamics can be applied directly, without consideration of the chemical potentials of the various atomic and molecular species that are present.

For our equilibrium Monte Carlo and molecular-dynamics calculations, we imposed the usual periodic boundary conditions in which the $N$-particle system is replicated throughout space by translation of the system by multiples of the edge lengths $L_x$, $L_y$, and $L_z$.

Our Monte Carlo technique is the usual Metropolis method [19] appropriate to the canonical ensemble. Thus we make a displacement of each of the atoms in turn (excluding the first), accepting the new configuration based on the change in potential energy of the system in accord with the so-called asymmetric transition probability. It should be observed in this regard that for temperatures that are low relative to the well depth of a given molecule $\varepsilon_{ab}/k_B$ a move which would dissociate the molecule would be rejected with virtual certainty. To achieve equilibrium at low temperatures, then, our Monte Carlo procedure will be ineffective, and procedures of the types discussed in the Introduction would be required [15–17].

In fact, for the quiescent explosive, we require the equation of state of the metastable system, not the equilibrium system, so that our Monte Carlo procedure can be expected to average the region of configuration space associated with the pure $AB$ system quite well. On the other hand, the state behind the detonation is expected to have thermal energy, which is only somewhat below that of the most stable species, say $\varepsilon_{AA}$. Thus the present scheme appears to serve quite well for both purposes, provided we do not attempt to study intermediate temperatures for which equilibration is too slow.

### C. Dynamics

The dynamics of our system consist of linear trajectories between binary "collisions." The latter include hard-sphere collisions, collisions with the repulsive core of the square well, and the interactions at the square-well boundary.

Consider the interaction of particle $i$ of species $s_i$ with particle $j$ of species $s_j$. We denote the position and velocity of particle $i$ by $\mathbf{r}_i$ and $\mathbf{v}_i$, respectively, and let

$$\mathbf{r}=\mathbf{r}_i-\mathbf{r}_j, \quad \mathbf{v}=\mathbf{v}_i-\mathbf{v}_j \ , \tag{5}$$

in which we simplify our notation (in this subsection only) by omitting subscripts on $\mathbf{r}$ and $\mathbf{v}$. Similarly, we denote $\sigma_{s_i s_j}$ by $\sigma$, $K_{s_i s_j}$ by $K$, $\varepsilon_{s_i s_j}$ by $\varepsilon$, and $m_{s_i}$ and $m_{s_j}$ by $m_i$ and $m_j$, respectively. Finally with respect to notation, we define $w$ to be the magnitude of $\mathbf{w}$ and $\hat{\mathbf{w}}$ to be the unit vector in the direction of $\mathbf{w}$.

We consider interactions between particles that are not bound to other particles and have, then, the square-well interaction potential of Eq. (1). We distinguish the various cases on the basis of the nature of the interaction. First, we define a type I interaction to be the hard-core collisions; it occurs only for particles that lie within the well $r<K\sigma$, approach each other $\mathbf{r}\cdot\mathbf{v}<0$, and lie in the collision cylinder of the core $r^2-(\mathbf{r}\cdot\hat{\mathbf{v}})^2<\sigma^2$. The collision then occurs at time,

$$t_c=-\frac{\mathbf{r}\cdot\hat{\mathbf{v}}+[\sigma^2-r^2+(\mathbf{r}\cdot\hat{\mathbf{v}})^2]^{1/2}}{v} \ , \tag{6}$$

yielding postcollision velocities that readily follow from the postcollision relative velocity,

$$\mathbf{v}'=\mathbf{v}+\Delta\mathbf{v} \ , \quad \Delta\mathbf{v}=-2(\mathbf{v}\cdot\hat{\mathbf{c}})\hat{\mathbf{c}} \ , \tag{7}$$

and the conservation of linear momentum,

$$m_i\mathbf{v}_i'+m_j\mathbf{v}_j'=m_i\mathbf{v}_i+m_j\mathbf{v}_j, \tag{8}$$

where

$$\mathbf{c}=\mathbf{r}(t_c) \tag{9}$$

is the line of centers at collision.

Secondly, we define interactions at the well boundary as type II interactions. We distinguish two subcases. (i) The atoms lie outside the well $r>K\sigma$, approached each other $\mathbf{r}\cdot\mathbf{v}<0$, lie in the collision cylinder of the well $r^2-(\mathbf{r}\cdot\hat{\mathbf{v}})^2<(K\sigma)^2$, and interact at time

$$t_c=-\frac{\mathbf{r}\cdot\hat{\mathbf{v}}+[(K\sigma)^2-r^2+(\mathbf{r}\cdot\hat{\mathbf{v}})^2]^{1/2}}{v} \ . \tag{10}$$

Evidently, the particles "associate" or bind by entering the well, with velocity change

$$\Delta\mathbf{v}=[-\mathbf{v}\cdot\hat{\mathbf{c}}+\sqrt{Q'}]\hat{\mathbf{c}} \ , \qquad Q'=(\mathbf{v}\cdot\hat{\mathbf{c}})^2+4\varepsilon/\mu \ , \quad \mu=\frac{2m_i m_j}{m_i+m_j} \ . \tag{11}$$

(ii) The atoms lie inside the well but do not have type I interactions, i.e., either they are receding, $\mathbf{r}\cdot\mathbf{v}>0$, or they approach but lie outside the collision cylinder of the core, $r^2-(\mathbf{r}\cdot\hat{\mathbf{v}})^2>\sigma^2$. Instead, they interact at the well boundary at time

$$t_c=\frac{-\mathbf{r}\cdot\hat{\mathbf{v}}+[(K\sigma)^2-r^2+(\mathbf{r}\cdot\hat{\mathbf{v}})^2]^{1/2}}{v} \ . \tag{12}$$

In this case, the particles reflect into the well if $Q<0$, where

$$Q=(\mathbf{v}\cdot\hat{\mathbf{c}})^2-4\varepsilon/\mu \ , \tag{13}$$

with velocity change Eq. (7). If $Q>0$, the molecule dissociates, with velocity change

$$\Delta\mathbf{v}=[-\mathbf{v}\cdot\hat{\mathbf{c}}+\sqrt{Q}\,]\hat{\mathbf{c}} \ . \tag{14}$$

The hard-sphere interaction applies for atoms, at least one of which is bound to a third atom. Provided the particles are approaching, $\mathbf{r}\cdot\mathbf{v}<0$, and lie within the collision cylinder $r^2-(\mathbf{r}\cdot\hat{\mathbf{v}})^2<(K\sigma)^2$, the collision time is given by the usual hard-sphere expression Eq. (10) for hard-core diameter $K\sigma$ and with velocity change given by Eq. (7).

### D. Monte Carlo molecular-dynamics procedure

Our calculations consist of a Monte Carlo average of functions of the phase $F(\underline{x}^N)$ determined from a sequence of points in phase space $\{\underline{x}_i^N; i=i,\ldots,N_{\mathrm{MC}}\}$, where

$$\underline{x}^N=\{\underline{r}^N,\underline{p}^N\} \ ,$$

$$\underline{p}^N=[\mathbf{p}_1,\mathbf{p}_2,\ldots,\mathbf{p}_N] \ .$$

The $\underline{r}_i^N$ form a realization of a Markov chain, generated by a Metropolis Monte Carlo procedure. Each such point in configuration space is combined with a point in momentum space, chosen randomly from the $N$-dimensional Maxwell-Boltzmann distribution using the Box-Muller method [20]. The resulting point in phase space $\underline{x}_i^N$ is used as an initial phase for a trajectory $\underline{x}_i^N(t)$ generated to a fixed number $N_t$ of time steps, each of length $\delta t$. The function $F(\underline{x}^N)$ is averaged in time over the trajectory, either as a sum over the discrete time steps or as an integral time average over the trajectory. The resulting time-averaged values are then averaged over the $N_{\mathrm{MC}}$ trajectories. The statistical uncertainties associated with the averages are determined from the variance over the $N_{\mathrm{MC}}$ trajectory averages.

As a practical matter, we typically generate the $(i+1)$th configuration through a standard Monte Carlo cycle from the final configuration of the $i$th trajectory rather than from the $i$th Monte Carlo configurations. Be-

cause energy is conserved on the trajectory, we are assured that the phase associated with this point has the same Boltzmann factor as that of the start of the trajectory. Moreover, the time-reversal invariance of the trajectory and the independence of the Boltzmann distribution on the sign of the velocities assures the microscopic reversibility of the overall Markov chain in phase space. The practical advantage is that the approach to equilibrium is more rapid in the combined procedure. At low temperatures especially, the approach can be rather slow [18].

## III. EQUILIBRIUM EQUATION OF STATE

Turning now to the detonation problem, we recall the classical equations [1] relating the quiescent state $(T_q, v_q)$ having mass velocity $u_q = 0$, with the state behind the detonation wave $(T, v, u)$,

$$\frac{D-u}{v} = \frac{D}{v_q} ,$$

$$p(T,v) - p_0(T_q, v_q) = \left[\frac{D}{v_q}\right]^2 (v_q - v) , \tag{15}$$

$$e(T,v) - e_0(T_q, v_q) = \tfrac{1}{2}[p(T,v) + p_0(T_q, v_q)](v_q - v) ,$$

in which $D$ is the detonation velocity, $e$ is the specific internal energy, and $p$ is the pressure; we add the subscript 0 to quantities for the metastable explosive. These constitute three equations in the four unknowns $T$, $v$, $u$ and $D$. The first of these equations can be regarded as determining the mass velocity in terms of the other three, leaving the second and third relations, the so-called "Rayleigh line" and the "Hugoniot curve," which can be regarded as two relations in two unknowns $T$ and $v$ parametrized by the detonation velocity. The Chapman-Jouguet hypothesis selects the solution having minimum detonation velocity as the solution for an "unsupported" detonation, i.e., a detonation wave in which the piston is ultimately brought to rest.

The third of Eq. (15), the Hugoniot curve, is seen to be independent of detonation velocity and is therefore the locus of possible final thermodynamic states behind a detonation wave. To evaluate it requires the specific internal energy and the pressure as functions of temperature and specific volume. The total internal energy in the canonical ensemble is given by the well-known expression

$$E(T,v) = \tfrac{3}{2} N k_B T + \langle U_N \rangle , \tag{16}$$

where the $\langle F \rangle$ denotes the ensemble average. While the pressure can be determined from two- and three-body distribution functions for a three-body potential [21], we instead evaluate the ensemble average of the *dynamical* pressure determined from the time-averaged momentum flux across a surface element in the system [22],

$$p_{\mathrm{MD}} = \frac{N k_B T_{\mathrm{MD}}}{V}\left[1 - \frac{\overline{W}_N}{\overline{\hat{K}}_N}\right] , \tag{17}$$

in which $p_{\mathrm{MD}}$ is dynamical pressure on a trajectory having dynamical temperature

$$T_{\mathrm{MD}} = \frac{2\overline{\hat{K}}_N}{3k_B N} , \tag{18}$$

$\hat{K}_N$ is the kinetic energy in the center-of-mass frame of reference,

$$\hat{K}_N = K_N - \frac{P^2}{2M}, \quad K_N = \tfrac{1}{2}\sum_i^N m_{s_i} v_i^2, \quad \mathbf{P} = \sum_i^N m_{s_i} \mathbf{v}_i , \tag{19}$$

$M$ is the total mass, and $W_N$ is the virial function, which for impulsive interactions is

$$W_N = -\tfrac{1}{2}\sum_\gamma m_{s_i} \mathbf{r}_{ij}(t_\gamma)\cdot\Delta\mathbf{v}_i(t_\gamma)\delta(t - t_\gamma) , \tag{20}$$

the $\gamma$ sum running over the successive interactions of the system at times $t_1, t_2, \ldots$. In Eq. (20), $i$ and $j$ denote the particles involved in the $\gamma$th interaction and $\Delta\mathbf{v}_i$ the velocity change of particle $i$. The overbar in Eq. (17) denotes the time average over the trajectory

$$\bar{f} = \lim_{t\to\infty} \frac{1}{t}\int_0^t f(\underline{x}^N(s))ds . \tag{21}$$

The determination of the Hugoniot curve consists, then, of the determination of the pressure and the internal energy at a series of temperatures for each value of the volume, to yield the Hugoniot function

$$h(T,v) = e(T,v) - e_0(T_q, v_q) - \tfrac{1}{2}[p(T,v) + p_0(T_q, v_q)](v_q - v) , \tag{22}$$

which can be interpolated to the roots of $h(T,v) = 0$.

In addition to computing the functions that enter into the Hugoniot function, we also count the various types of collisions. From these, we compute the mean free times for five types of events. (i) The intermolecular mean free time $t_0^{(m)}$ is defined as the time between repulsive collisions of a bound atom and any other atom outside the molecule, inasmuch as collisions of free atoms always result in the formation of a molecule. We compute $t_0^{(m)}$ from the hard-sphere collision rate $\Gamma^{(\mathrm{hs})}$ by noting that in time $t_0^{(m)}$ (ignoring any distinction between the two classes of events involved) *each* particle will have undergone one such collision, on the average. We therefore define $t_0^{(m)}$ to be the time for $2\langle N_{\mathrm{mol}}\rangle(N-2)/(2N)$ such collisions and we write

$$t_0^{(m)} = \frac{\langle N_{\mathrm{mol}}\rangle(N-2)}{N\langle \Gamma^{(\mathrm{HS})}\rangle} , \tag{23}$$

in which $N_{\mathrm{mol}}$ is the number of molecules. (ii) The mean free time between intramolecular hard-core collisions follows similarly from the collision rate $\Gamma^{(c)}$ for such collisions,

$$t_0^{(c)} = \frac{\langle N_{\mathrm{mol}}\rangle}{\langle \Gamma^{(c)}\rangle} . \tag{24}$$

(iii) The mean free time between intramolecular reflections from the well wall is similarly written

$$t_0^{(w)} = \frac{\langle N_{\rm mol} \rangle}{\langle \Gamma^{(w)} \rangle} \ . \tag{25}$$

(iv) The mean free time between dissociative events is written

$$t_0^{(\rm ds)} = \frac{\langle N_{\rm mol} \rangle}{\langle \Gamma^{(\rm ds)} \rangle} \ . \tag{26}$$

(v) The mean free time between associative events is

$$t_0^{(\rm as)} = \frac{\langle N_{\rm atm} \rangle - 1}{2\langle \Gamma^{(\rm as)} \rangle}, \tag{27}$$

in which $N_{\rm atm}$ is the number of free atoms. We note that the frequencies of events of the latter two types should balance at equilibrium,

$$\langle \Gamma^{(\rm ds)} \rangle = \langle \Gamma^{(\rm as)} \rangle \ .$$

Each of these five quantities defines a time scale for a distinct fundamental process.

## IV. CALCULATIONS

We describe now the specific calculations that are reported here, including the parameters of the interaction potential, the thermodynamic state of the quiescent system, the details of the time averaging, the initial phase for the equation-of-state calculations, and the general nature of the statistical analysis of our results.

### A. Specification of problem

We consider the system defined by the following parameters:

$$\begin{aligned} &m_B = \tfrac{15}{64} m_A \ , \\ &\sigma_B = \sigma_A \ , \\ &K_{AA} = K_{AB} = 3 \ , \\ &K_{BB} = 1.1 \ , \\ &\varepsilon_{AA} = 3\varepsilon_{AB} \ , \\ &\varepsilon_{BB} = \varepsilon_{AB} \ , \end{aligned} \tag{28}$$

so that the heat of the reaction

$$2AB \rightleftharpoons A_2 + B_2 \tag{29}$$

is $\varepsilon_{AB}$ per molecule of reactant. For the quiescent state of the system we choose a volume of $7V_0$ in which $V_0$ is the volume of a close-packed system of $N/2$ hard spheres of diameter $K_{AB}\sigma_{AB}$, viz.,

$$V_0 = \frac{\sqrt{2}}{4} N (K_{AB}\sigma_{AB})^3 \ . \tag{30}$$

The quiescent temperature is $0.05\varepsilon_{AB}/k_B$, so that the heat of reaction is 20 times the thermal energy in the quiescent fluid.

### B. Molecular-dynamics averaging

The dynamical trajectory is generated through a computer program that proceeds from "event to event;" that is, the program determines a minimum time for each particle, namely, the earliest time for which an interaction with another particle takes place, based on the interaction types discussed in Sec. II. In order to minimize the number of such interactions that need to be considered, the program uses cell tables whereby only interactions with particles in neighboring cells need to be calculated. New interaction times for a particle need to be calculated only after that particle changes cells or undergoes an interaction.

At intervals of time $\delta t$ the functions of the phase, for example, the potential energy, are evaluated to form a trajectory average. The microscopic pressure Eqs. (17)–(20), however, involves $\delta$ functions in the time and is evaluated through the integral-time average Eq. (21) as a sum over interactions. The time $\delta t$ is chosen to be

$$\delta t = 0.1 t^* \ , \tag{31}$$

in which $t^*$ is a crude approximation to the intermolecular mean free time of the system, viz., the low-density Boltzmann mean free time for $N/2$ hard spheres of mass $m_A + m_B$ and equal in volume to the $AB$ molecular volume,

$$t^* = \frac{2V}{N(2\sigma)^2} \left[ \frac{(m_A + m_B)\beta}{\pi} \right]^{1/2} , \quad \sigma^3 = \sigma_A^3 + \sigma_B^3 \ , \tag{32}$$

where $\beta = 1/(k_B T)$. For each system, the trajectories were extended to the same number $N_t$, time steps $N_t = 3000$, before beginning a new Monte Carlo cycle.

### C. Initialization of the phase

The initial configuration of the system for each state $(T, v)$ is ultimately derived from a face-centered-cubic lattice of $AB$ molecules for the quiescent state. That configuration consists of $A$ atoms occupying the lattice sites with a $B$ atom attached to each $A$ at a random radial position within the attractive well, at a latitudinal angle with respect to the $x$ axis chosen randomly in a narrow range about $\pi/4$ and with a longitudinal angle of $\pi/4$.

For densities greater than the quiescent state, the initial configuration was derived from the final configuration for a neighboring state, using either uniform expansion or contraction of the system to effect any required change in density. In the case of contraction, the density is increased in steps as permitted by the nearest pair of particles, with a number of Monte Carlo moves used to "equilibrate" between each contraction. For systems in which the primary cell has edge lengths that are multiples of those for smaller systems at the same state point, the initial configuration was derived from the final configuration of the smaller system by filling the larger cell with translated copies of the smaller.

### D. Analysis of the results

The calculations produce a series of values for the pressure and the potential energy, one for each trajectory. In many cases, the first few trajectories appear not near equilibrium, as seen from the trajectory-averaged values of the potential energy. We ignore these trajectories in computing our overall averages and estimates for the statistical uncertainty. In order to assure the absence of appreciable serial correlations between successive trajectory averages, we apply a number of the standard test of randomness [23].

## V. RESULTS

We have studied the system described above at the quiescent state $V_q=7V_0$, $T_q=0.05\varepsilon/k_BT$, as well as for six values of the volume between $6V_0$ and $4V_0$ for a range of temperatures between $4T_q$ and $7.6T_q$. The states that were studied are listed in Table I, which includes several

TABLE I. Parameters and results for Monte Carlo molecular-dynamic calculations of the equilibrium properties of equimolar mixtures of $A$ and $B$ particles interacting through the reactive square-well hard-sphere potential for the various values of the volume $V$, relative to the reference volume $V_0$, Eq. (30), and temperature $T$, relative to the depth $\varepsilon_{AB}$ of the potential well of the $AB$ molecule: $N$ is the total number of particles in the system; $N_{MC}$ is the number of distinct trajectories generated, of which the last $n_{MC}$ yields statistically independent estimates of the thermodynamics functions of the mixture; $N_{int}$ is the total number of interactions, in millions, computed for all trajectories; $pV/Nk_BT$ is the compressibility factor; and $\langle U\rangle$ is the average potential energy. Each trajectory extends to 3000 time steps $\delta t$, Eq. (31), except those for the metastable, molecular $AB$ state, $V=7V_0$, $T=0.05\varepsilon_{AB}/k_B$, which extend to 300 time steps per trajectory. The numbers in parentheses are the standard deviations, relative to the low-order digit of the mean values.

| $\frac{V}{V_0}$ | $\frac{k_BT}{\varepsilon_{AB}}$ | $N$ | $N_{MC}$ | $n_{MC}$ | $N_{int}$ | $\frac{pV}{Nk_BT}$ | $-\frac{\langle U\rangle}{Nk_BT}$ |
|---|---|---|---|---|---|---|---|
| 7 | 0.05 | 216 | 100 | 90 | 7.5 | 1.1958(4) | 10.0000(0) |
| 6 | 0.20 | | 30 | 11 | 73.2 | 1.2765(59) | 4.4190(160) |
| | 0.24 | | 30 | 19 | 59.8 | 1.3325(39) | 3.4591(110) |
| | 0.26 | | 40 | 20 | 73.8 | 1.3562(30) | 3.1774(70) |
| | 0.28 | | 33 | 26 | 55.8 | 1.3774(33) | 2.8945(77) |
| | 0.30 | | 30 | 20 | 45.7 | 1.4054(41) | 2.6134(55) |
| 5.2 | 0.24 | 216 | 29 | 22 | 56.7 | 1.4574(47) | 3.5311(97) |
| | 0.26 | | 30 | 30 | 54.2 | 1.4917(41) | 3.2083(89) |
| | 0.28 | | 30 | 21 | 50.6 | 1.5096(43) | 2.9427(78) |
| | 0.30 | | 30 | 21 | 46.6 | 1.5278(44) | 2.7021(100) |
| | 0.34 | | 30 | 20 | 39.7 | 1.5633(37) | 2.3031(70) |
| 5 | 0.20 | 216 | 30 | 15 | 67.9 | 1.4308(64) | 4.4660(100) |
| | | 1728 | 20 | 20 | 381.0 | 1.4224(14) | 4.4874(32) |
| | 0.24 | 216 | 30 | 21 | 58.6 | 1.4838(52) | 3.5905(91) |
| | | 1728 | 30 | 20 | 471.9 | 1.4937(21) | 3.5660(32) |
| | 0.30 | 216 | 40 | 30 | 61.1 | 1.5776(37) | 2.6795(76) |
| | | 1728 | 22 | 13 | 269.4 | 1.5670(17) | 2.6967(34) |
| | 0.32 | 216 | 30 | 18 | 42.9 | 1.6028(52) | 2.4824(61) |
| | | 1728 | 20 | 14 | 226.7 | 1.5907(12) | 2.4819(28) |
| | 0.34 | 216 | 30 | 14 | 58.6 | 1.6126(40) | 2.3018(53) |
| | | 1728 | 20 | 20 | 210.7 | 1.6061(15) | 2.2925(26) |
| 4.8 | 0.24 | 216 | 30 | 21 | 58.6 | 1.5416(47) | 3.5934(72) |
| | 0.28 | | 30 | 10 | 49.7 | 1.5967(38) | 2.9613(100) |
| | 0.30 | | 30 | 23 | 45.8 | 1.6218(51) | 2.6953(72) |
| | 0.32 | | 30 | 26 | 42.6 | 1.6403(49) | 2.4835(77) |
| | 0.34 | | 30 | 30 | 40.3 | 1.6574(48) | 2.3200(70) |
| 4.6 | 0.24 | 216 | 30 | 19 | 57.3 | 1.5939(36) | 3.5794(54) |
| | 0.26 | | 30 | 25 | 53.7 | 1.6138(48) | 3.2686(61) |
| | 0.28 | | 30 | 26 | 49.1 | 1.6402(49) | 2.9807(80) |
| | 0.30 | | 30 | 25 | 46.1 | 1.6672(58) | 2.7163(95) |
| | 0.32 | | 30 | 16 | 42.9 | 1.6933(53) | 2.5254(62) |
| | 0.34 | | 30 | 19 | 40.0 | 1.7151(73) | 2.3095(88) |
| 4 | 0.20 | 216 | 40 | 18 | 82.3 | 1.6660(36) | 4.6073(67) |
| | 0.24 | | 40 | 16 | 73.5 | 1.7625(99) | 3.6811(110) |
| | 0.30 | | 30 | 24 | 45.1 | 1.8595(46) | 2.7524(56) |
| | 0.34 | | 20 | 10 | 26.7 | 1.9193(100) | 2.3378(91) |
| | 0.38 | | 30 | 28 | 36.7 | 1.9447(59) | 2.0649(52) |

parameters of importance, including the number of particles $N$. Note that only for a volume of $5V_0$ have we studied systems of 1728 particles; otherwise we have treated 216 particles. The table also lists the total number of interactions $N_{\rm int}$ encountered for the $N_{\rm MC}$ trajectories. As previously noted, the first few trajectories tend to sample regions of phase space rather far from equilibrium, so only the final $n_{\rm MC}$ of these trajectories are used in computing averages and statistical uncertainties of the thermodynamic functions. The values of $N_{\rm MC}$ and $n_{\rm MC}$ are also given in Table I. The number of trajectories discarded depends on the details of the starting configuration, which typically was representative of equilibrium for a nearby state point.

A case of slow approach to equilibrium is illustrated in Fig. 1 for the system $T=0.2\varepsilon_{AA}/k_B$, $V=4.0V_0$, the starting configuration of which was the final configuration of the twentieth trajectory of a $T=0.1\varepsilon_{AA}/k_B$ realization at the same volume. We see the very gradual approach to equilibrium of the average potential energy on successive trajectories. Thus, we choose $n_{\rm MC}=18$, discarding the first 22 trajectories of Fig. 1. These final 18 trajectory averages give no indication of further serial correlation and appear to be normally distributed on the basis of, for example, the mean-square–successive-difference ratio test [23].

For temperatures appreciably below $0.2\varepsilon_{AA}/k_B$, the rate of the chemical reactions appears to be so slow that the present Monte Carlo molecular-dynamics method becomes rather ineffective in reaching the "equilibrium" regions of phase space. This equilibration "phase" is a familiar feature of Monte Carlo and molecular-dynamics simulations but is here controlled by chemical reaction rather than the relatively rapid thermal transport processes. Thus the 22 "discarded" trajectories of Fig. 1 include $1.9\times10^6$ MC moves and $4.5\times10^7$ collisions, values that are many orders of magnitude larger than would be required, for example, to equilibrate a system of hard spheres at a similar density. For the systems of 1728 atoms, the fluctuations (relative to mean values) are smaller than for the 216 atoms, so that the approach to equilibrium is effectively slower. Perhaps the Monte Carlo procedures discussed in Sec. I would be more appropriate for these temperatures.

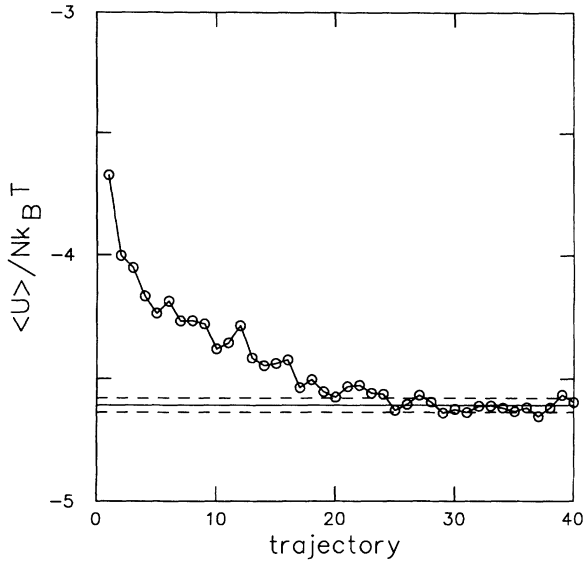


FIG. 1. Average potential energy per particle for the 40 trajectories of an equimolar reactive mixture of $A$ and $B$ atoms at a volume of four times the reference volume $V_0$, Eq. (30), and temperature $0.20\varepsilon_{AB}/k_B$. The solid horizontal line marks the mean of the final 18 trajectories, and the dashed lines mark one standard deviation above and below the mean.

### A. Thermodynamic functions

The equilibrium composition was determined for each state point through the mole fraction of each of the 5 distinct components, viz., free atoms $A$ and $B$, and three distinct molecular species. Note that the present model avoids the ambiguity in identifying molecules, inherent in many classical models of chemical reaction based on soft interactions. The mole fractions of the principal species, free $B$ atoms and $AA$ molecules, are shown as functions of temperature and volume in Figs. 2(a) and 2(b), respectively. The data for each volume are fitted to a quadratic function in the temperature, for $T\geq0.24\varepsilon/k_B$, of the form

$$f(T,v)=a_f(v)+b_f(v)\left[\frac{k_BT}{\varepsilon_{AB}}\right]+c_f(v)\left[\frac{k_BT}{\varepsilon_{AB}}\right]^2. \qquad (33)$$

The fitted curves for the mole fractions are shown in the figures. The mole fraction of free $A$ atoms is no more than 0.005 for the entire range of volume and temperature covered in these calculations. The mole fraction of $AB$ molecules is much higher but remains in the range $\{0.02,0.1\}$ throughout. Finally, the mole fraction of $BB$ molecules lies in the range $\{0.09,0.31\}$, decreasing with increasing temperature and volume. On the other hand,

TABLE II. The Hugoniot temperature ratio $T_h(v)/T_q$, pressure ratio $p_h(v)/p_q$, and detonation velocity $D$ as functions of reduced volume $V/V_0$ for the square-well hard-sphere interaction having interaction parameters Eq. (28) for the quiescent state $V_q=7V_0$, $T_q=0.05\varepsilon_{AB}/k_B$.

| $\frac{V}{V_0}$ | $N$ | $\frac{T_h}{T_q}$ | $\frac{p_h}{p_q}$ | $D\left[\frac{(m_A+m_B)}{k_BT_q}\right]^{1/2}$ |
|---|---|---|---|---|
| 6 | 216 | 5.578(10) | 7.495(26) | 10.428(14) |
| 5.2 | 216 | 6.022(14) | 10.39(4) | 0.344(13) |
| 5 | 216 | 6.083(13) | 11.25(4) | 9.263(13) |
| | 1728 | 6.099(6) | 11.24(2) | 9.257(6) |
| 4.8 | 216 | 6.217(15) | 12.37(5) | 9.303(14) |
| 4.6 | 216 | 6.405(13) | 13.80(5) | 9.449(12) |
| 4 | 216 | 7.011(21) | 19.72(10) | 10.220(19) |

the mole fraction of $AB$ increases slightly with temperature and decreases with volume over the range of our calculations.

The compressibility factor and the potential energy per particle are given in Table I, and are plotted against temperature and volume in Figs. 2(c) and 2(d). The curves in the figures are fits of the form of Eq. (33), but omitting the quadratic term in those cases where the data are sufficiently linear. The reduced potential energy per particle, shown in Fig. 2(d), is seen to be nearly independent of volume over the range studied. We recognize, of course, that our analytic representation are expected to fail outside the temperature range of the fit. The effect of system size can be seen from the $V=5V_0$ results in Table I to be small and of marginal statistical significance with respect to any of our observations.

The time scales at which various collisions take place are summarized by the mean free times for each of the five types of events discussed in Sec. III. We plot three of these, the intermolecular $t_0^{(m)}$ and the intermolecular $t_0^{(c)}$ and $t_0^{(ds)}$, as functions of volume and temperature in Fig. 3. These values were estimated by averaging the values for the individual trajectories given by Eqs. (23)–(27). We see that over the limited state space of these calculations, the intermolecular mean free time is roughly $0.09t^*$, the intramolecular times $t_0^{(c)}$ are about half that, while the dissociation times are the longest, ranging from about $4t^*$ at $T=0.2\varepsilon_{AB}/k_B$ to less than $t^*$ at the higher temperatures. The recombination times also decrease with increasing temperature, although not so rapidly.

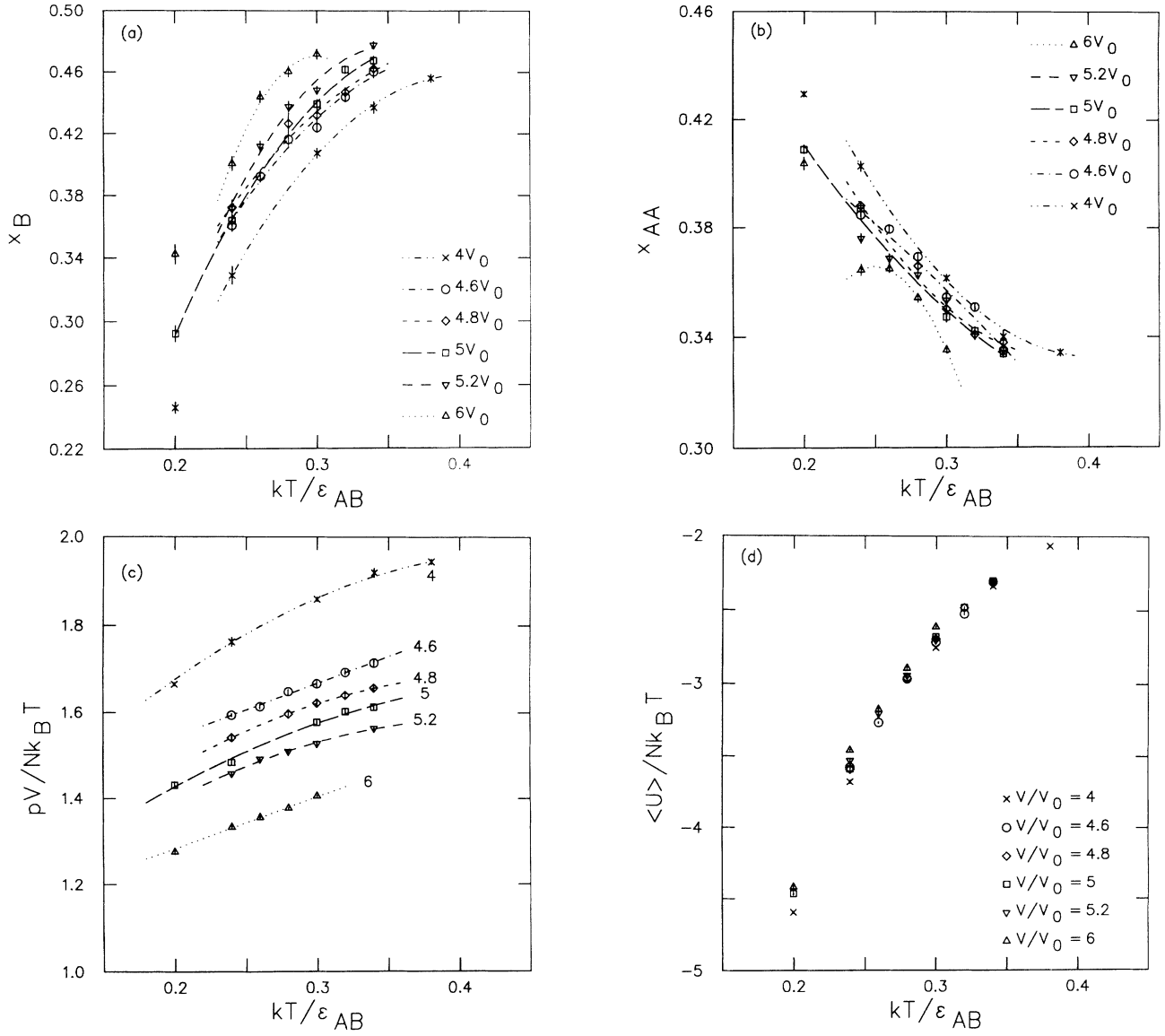


FIG. 2. Mole fraction of (a) free $A$ atoms $x_A$ and (b) $BB$ molecules $x_{BB}$, (c) the compressibility factor $pV/Nk_BT$, and (d) the reduced average potential energy per particle $\langle U\rangle/Nk_BT$ of equimolar reactive mixtures of $A$ and $B$ atoms as functions of temperature for six values of the volume $V$ relative to the reference volume $V_0$, Eq. (30). The curves are least-squares fits to the data.

### B. Hugoniot curve

The function $h(T,v)$, Eq. (22), can be computed directly from the Monte Carlo molecular-dynamics values of the internal energy and pressure, thereby obtaining a set of time-averaged values that can be fitted, for each value of the volume, to a quadratic in the temperature, similar to the least-squares-fitting procedure above. It can also be evaluated from the analytic representations for the average potential energy and pressure; the results via either path are virtually indistinguishable. Using the direct least-squares fit, we solve the resulting quadratic in the temperature for the Hugoniot point,

$$h(T,v)=0\ , \tag{34}$$

namely, $T=T_h(v)$, from which we also compute $p_h(v)$ through Eq. (33). For our six values of the volume and two values of the system size, we obtain the Hugoniot states shown in Table II and the pressure-volume Hugoniot "curve" shown in Fig. 4 for the 216-particle systems; the dotted line in the figure is a spline fit to the points.

The detonation velocity corresponding to each Hugoniot point is obtained from the second line of Eq. (28) and the values are also listed in Table II. The 1728-particle value is seen to lie close to that for 216 particles. The tangent to the Hugoniot curve through the quiescent state $(v_q,p_q)$ yields then the CJ detonation velocity. The least-squares fit of $D$ to a quadratic in the volume yields at the minimum,

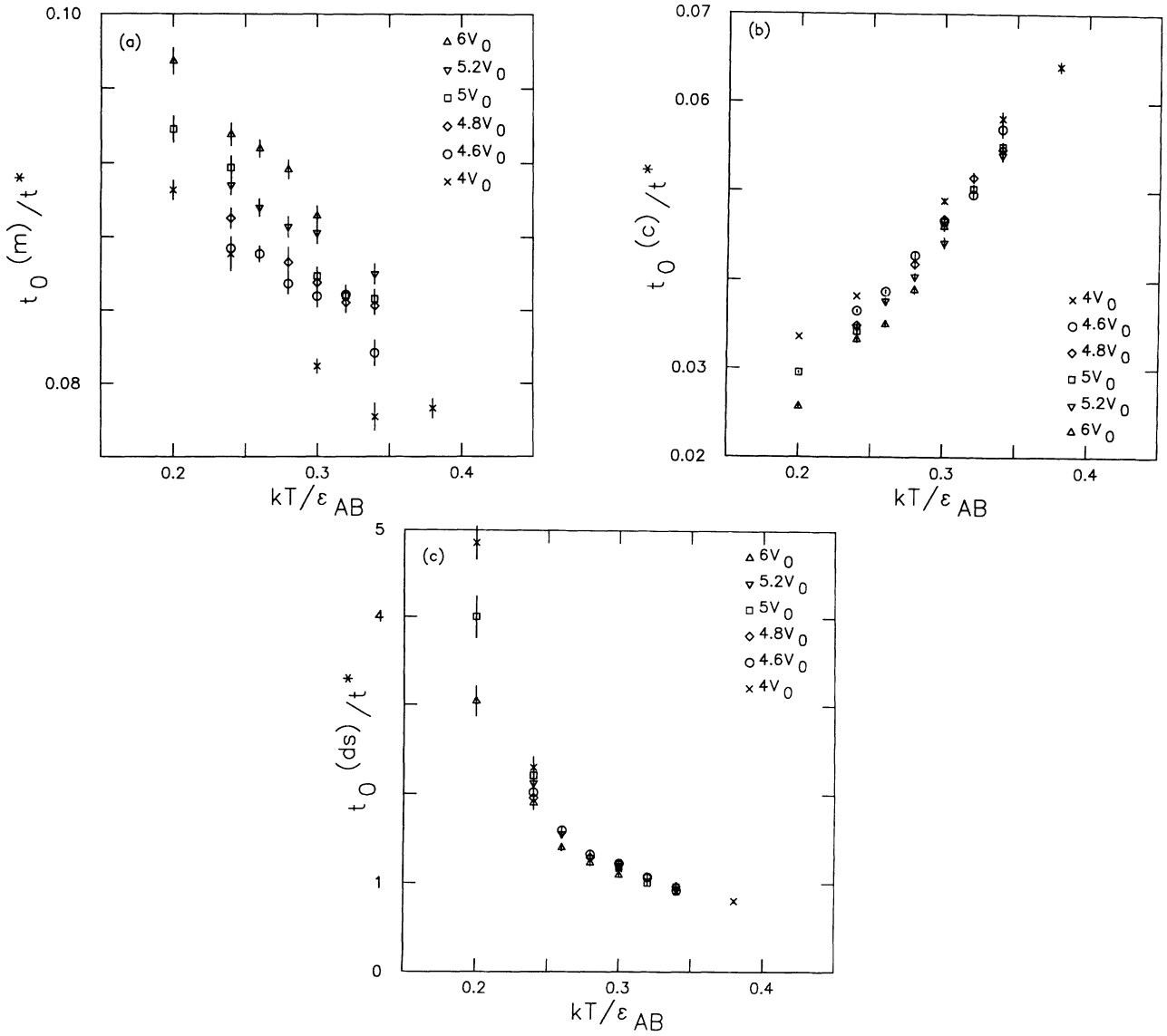


FIG. 3. Mean free time $t_0^{(\alpha)}$ for three types of events for equimolar reactive mixtures of $A$ and $B$ atoms as functions of temperature for six values of the volume $V$ relative to the reference volume $V_0$, Eq. (30): (a) $\alpha=m$, intermolecular collisions; (b) $\alpha=c$, intramolecular collisions at the molecular core, irrespective of the type of molecule, and $\alpha=ds$, for intramolecular dissociating events.

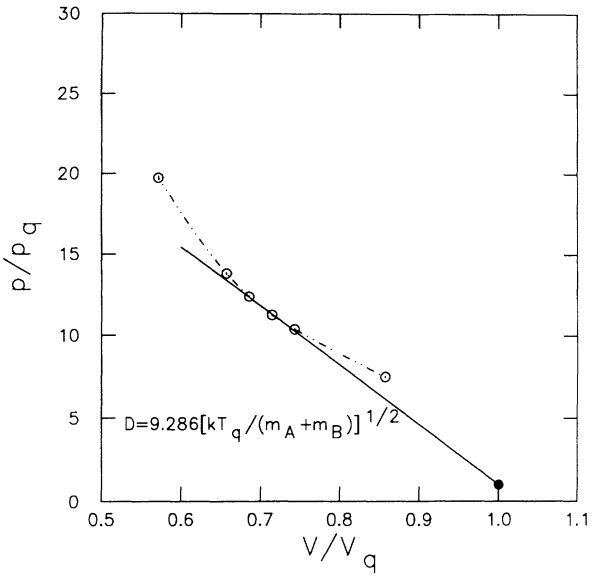


FIG. 4. Hugoniot curve (dotted) for the quiescent state $V_q=7V_0$, $T_q=0.05\varepsilon_{AB}/k_B$ and the Chapman-Jouguet Rayleigh line (solid), tangent to that curve.

$$V_{\mathrm{CJ}}=(4.96\pm0.13)V_0\ ,$$
$$D_{\mathrm{CJ}}=(9.286\pm0.006)\left[\frac{k_BT_q}{m_A+m_B}\right]^{1/2}\ . \tag{35}$$

## VI. DISCUSSION

The square-well hard-sphere fluid is found to yield a Hugoniot curve of the form expected for an explosive, with a CJ detonation velocity that seems reasonable for the rather low density we have considered for the quiescent state.

The principle difference between the present approach and those based on nonreactive potentials is our use of a combination of Monte Carlo and molecular dynamics to determine the thermodynamic functions, rather than a Monte Carlo procedure in which the Markov chain incorporates changes in molecular composition explicitly. Rather, in the present approach the Monte Carlo aspect of our calculation basically provides statistically independent estimates of the thermodynamics functions, acting then principally as a device for estimating statistical uncertainties of our results. The present approach depends strongly on the existence of a dynamical path in phase space from the starting configuration to the equilibrium composition. As we see at lower temperature, the time needed to reach equilibrium can be quite large. It would seem that the convergence of our results could well have been improved by incorporating atomic exchanges in the Monte Carlo as well.

The goal of the present calculations is that of setting the stage for nonequilibrium calculations of detonation waves by determining the predictions of the classical theory of detonation. These nonequilibrium calculations are currently in progress.

[1] R. Courant and K. O. Friedrichs, *Supersonic Flow and Shock Waves* (Interscience, New York, 1948).
[2] D. R. White, Phys. Fluids **4**, 465 (1960).
[3] J. J. Erpenbeck, Phys. Fluids **7**, 684 (1964).
[4] J. J. Erpenbeck, Phys. Fluids **9**, 1293 (1966).
[5] W. Fickett and W. C. Davis, *Detonation* (University of California Press, Berkeley, 1979).
[6] C. L. Mader, *Numerical Modeling of Detonation* (University of California Press, Berkeley, 1979).
[7] A. M. Karo, J. R. Hardy, and F. E. Walker, Acta Astron. **5**, 1041 (1978).
[8] D. H. Tsai and S. F. Trevino, J. Chem. Phys. **81**, 5636 (1984).
[9] M. Peyrard, S. Odiot, E. Lavenir, and J. M. Schnur, J. Appl. Phys. **57**, 2626 (1985).
[10] M. Peyrard, S. Odiot, E. Oran, J. Boris, and J. Schnur, Phys. Rev. B **33**, 2350 (1986).
[11] P. Maffre and M. Peyrard, Phys. Rev. B **45**, 9551 (1992).
[12] M. L. Elert, D. M. Deaven, D. W. Brenner, and C. T. White, Phys. Rev. B **39**, 1453 (1989).
[13] D. H. Robertson, D. W. Brenner, M. L. Elert, and C. T. White (unpublished).
[14] S. G. Lambrakos, M. Peyrard, E. S. Oran, and J. P. Boris, Phys. Rev. B **39**, 993 (1989).
[15] D. F. Coker and R. O. Watts, Mol. Phys. **44**, 1303 (1981).
[16] D. A. Kofke and E. D. Glandt, Mol. Phys. **64**, 1105 (1988).
[17] M. S. Shaw, J. Chem. Phys. **94**, 7550 (1991).
[18] F. H. Stillinger, T. A. Weber, and R. A. LaViolette, J. Chem. Phys. **85**, 6460 (1986).
[19] W. W. Wood, in *Physics of Simple Liquids*, edited by H. N. V. Temperley, J. S. Rowlinson, and G. S. Rushbrooke (North-Holland, Amsterdam, 1968) p. 116.
[20] W. J. Kennedy and J. E. Gentile, *Statistical Computing* (Dekker, New York, 1980).
[21] F. H. Stillinger, in *Nonsimple Liquids*, edited by I. Prigogine and S. A. Rice (Wiley, New York, 1975), p. 1.
[22] J. J. Erpenbeck and W. W. Wood, in *Statistical Mechanics, Part B, Time Dependent Processes*, Vol. 6 of Modern Theoretical Chemistry, edited by B. J. Berne (Plenum, New York, 1977), p. 1.
[23] A. Hald, *Statistical Theory with Engineering Applications* (Wiley, New York, 1952).